

RESEARCH

Open Access



# Aniline TFPA enhances camptothecin-induced anti-NSCLC by modulating oxidative stress and impairing autophagy

Han-Lin Chou<sup>1†</sup>, I-Ling Lin<sup>2,3†</sup>, Yei-Tsung Chen<sup>4</sup>, Wen-Tsan Chang<sup>5,6,7</sup>, Ann Yu<sup>1</sup>, Wei-Chun Chen<sup>1</sup>, Chang-Yi Wu<sup>1,8</sup>, Shean-Jaw Chiou<sup>9</sup>, Chih-Wen Shu<sup>10</sup>, Chien-Chih Chiu<sup>1,7,8,11,12\*</sup> and Pei-Feng Liu<sup>13\*</sup>

## Abstract

**Background** Camptothecin (CPT) derivatives are widely used in cancer therapies, but their efficacy can be attenuated by resistance mechanisms such as autophagy. We recently showed that the aniline compound 4-[4-(4-aminophenoxy)-2,3,5,6-tetrafluorophenoxy] aniline (TFPA) can potently increase CPT cytotoxicity against non-small cell lung cancer (NSCLC) cells. The purpose of this study was to evaluate whether TFPA improves CPT-based chemotherapy by modulating autophagy and other cell death pathways in NSCLC models.

**Methods** Two NSCLC cell lines, A549 and H1299, were tested. The synergism of CPT and TFPA was evaluated by trypan blue exclusion and colony formation assays. Annexin V staining was used for the detection of apoptosis, and autophagy was assessed by acridine orange staining and immunofluorescence. Flow cytometry-based dihydroethidium staining was used to assess oxidative stress. Changes in the expression of apoptosis-associated factors and autophagy-associated factors were determined by Western blot assays. The synergism of CPT and TFPA was validated using a zebrafish xenograft assay.

**Results** The accumulation of markers for lysosomal expansion (LAMP2) and degradation (cathepsin D) and markers for autophagosome formation (LC3B-II) suggested that blockage of autolysosome formation might impair autophagy in CPT-treated NSCLC cells and subsequently lead to autophagic cell death. Cotreatment with TFPA and CPT induced cell death by increasing the production of reactive oxygen species, which contributed to autophagic impairment and eventually apoptotic cell death in NSCLC cells.

**Conclusions** Our present work suggests that increased autophagic impairment induced by the combination of CPT and TFPA contributes to the apoptotic cell death of lung cancer cells.

**Keywords** Lung cancer, Autophagy impairment, CPT, Aniline, TFPA, Oxidative stress

<sup>†</sup>Han-Lin Chou and I-Ling Lin contributed equally to this work.

\*Correspondence:  
Chien-Chih Chiu  
cchiu@kmu.edu.tw  
Pei-Feng Liu  
pflu@kmu.edu.tw

Full list of author information is available at the end of the article



© The Author(s) 2025. **Open Access** This article is licensed under a Creative Commons Attribution-NonCommercial-NoDerivatives 4.0 International License, which permits any non-commercial use, sharing, distribution and reproduction in any medium or format, as long as you give appropriate credit to the original author(s) and the source, provide a link to the Creative Commons licence, and indicate if you modified the licensed material. You do not have permission under this licence to share adapted material derived from this article or parts of it. The images or other third party material in this article are included in the article's Creative Commons licence, unless indicated otherwise in a credit line to the material. If material is not included in the article's Creative Commons licence and your intended use is not permitted by statutory regulation or exceeds the permitted use, you will need to obtain permission directly from the copyright holder. To view a copy of this licence, visit <http://creativecommons.org/licenses/by-nc-nd/4.0/>.

## Background

Lung cancer is one of the leading causes of death in the United States and Asia [1, 2]. Non-small cell lung cancer (NSCLC) is the most common type of lung cancer, and it is estimated that more than 80% of lung cancers are NSCLC. In recent decades, with advances in medicine, different therapies have been developed according to the stage of NSCLC. To date, chemotherapy remains the most common treatment for NSCLC patients. Several anti-lung cancer drugs, such as cisplatin [3], irinotecan [4], and topotecan [5], have been used for cancer treatment and have shown beneficial effects on cancer patients. Nevertheless, the development of chemoresistance after monotherapy for NSCLC patients remains a major concern in the field because it not only attenuates the efficacy of the drug but also contributes to poor prognosis and high recurrence rates [6–8]. Thus, the development of combination chemotherapy, treatment with two or more drugs, has been evolving as one of the main anti-cancer strategies designed to improve the survival rate of various cancers, including NSCLC [5, 9, 10]. For example, Niho et al. found that irinotecan enhances the efficacy of cisplatin in large-cell neuroendocrine carcinoma [11]. Therefore, combination chemotherapy is considered a promising strategy for lung cancer treatment.

Camptothecin (CPT), a cytotoxic quinoline alkaloid compound, was originally isolated from *Camptotheca acuminata* [12]. CPT and its derivatives are widely used to treat cancers, including lung cancer [13], liver cancer [14], and colorectal cancer [15], because they have been shown to exert multiple anticancer effects, including suppression of proliferative activity [16], induction of apoptosis [16, 17], and alteration of autophagy responses [18]. However, drug resistance limits the efficacy of CPT-based drugs, such as topotecan and irinotecan, in NSCLC patients [19]. Some studies have indicated that autophagy might be associated with drug resistance in cancer cells, such as lung cancer cells [20, 21]. Importantly, in colorectal and lung cancer cells, a low dose of CPT induces protective autophagy and concomitantly attenuates the induction of apoptosis in cancer cells [22, 23]. Recent studies have also suggested that the combination of autophagy modulators with chemotherapy could be a novel approach for developing future anti-lung-cancer strategies [22, 24, 25].

Autophagy is a highly conserved degradation system in eukaryotic cells that has been shown to eliminate unnecessary organelles and damaged proteins [26]. The autophagy process includes at least four stages: initiation, elongation, maturation, fusion of lysosomes and autophagosomes to form autolysosomes, and final degradation of damaged organelles or macromolecules [27]. Recent studies have demonstrated that autophagy may be correlated with the chemoresistance of cancer cells [28].

In two separate studies, researchers have demonstrated that CPT- or topotecan-induced autophagy promotes colorectal cancer cell survival [22, 29], which suggests that chemotherapy-induced autophagy might be a complementary survival mechanism that protects cancer cells from apoptosis. Accumulating evidence suggests that disruption of the autophagy process may further enhance chemotherapy-induced apoptosis in cancer cells. For instance, the inhibition of autophagy by 3-methyladenine (3-MA) enhances cisplatin-induced apoptosis in A549 lung cancer cells [30]. Additionally, chloroquine (CQ), an autophagy inhibitor, enhances CPT-induced apoptosis in two colorectal cancer cell lines, HCT116 and RKO, by disrupting the autophagy process [22].

Aniline, a primary aromatic amine, has been reported to exert various bioactivities, including anticancer [31], antifungal [32], and anti-inflammatory activities [33]. An aniline-containing compound, 11 $\beta$  (CAS 865070-37-7), reportedly induces apoptosis in both prostate cancer LNCaP cells [34] and cervical cancer HeLa cells [35]. Another aniline derivative, acetaminophen, has been reported to induce cytotoxicity in hepatocellular cancer HepG2 cells and lead to cell death [36, 37]. Combination therapy with aniline derivatives and other drugs was recently shown to significantly enhance the efficacy of monotherapy. One study identified that 4-(2-cyclohexylethoxy) aniline (IM3829) as an aniline derivative that enhances radiation-induced cell death in human lung cancer H1299 cells [38]. In addition, Bonnet et al. reported that pyridyl aniline thiazole, an aniline-containing compound, exerts inhibitory effects on renal carcinoma RCC4 cells by modulating autophagy processes [39].

The induction of autophagy by chemotherapy has been reported to protect cancer cells from the cytotoxic effect of drugs [40], such as CPT or its derivatives [22, 41, 42]. To overcome these issues, the inhibition or disruption of the autophagy process has been indicated to enhance chemotherapy-induced apoptosis of cancer cells [43].

In this study, we identified the aniline-containing compound 4-[4-(4-aminophenoxy)-2356-tetrafluorophenoxy] aniline (TFPA), and using both a cell model and a zebrafish xenograft model, we found that this compound has low cytotoxicity and enhances cell death in CPT-treated NSCLC cells. Furthermore, TFPA enhanced the CPT-induced proliferation inhibition and cell death in NSCLC cells by modulating the level of endogenous reactive oxygen species (ROS) and subsequently impaired autophagy, as evidenced by the nuclear retention of microtubule-associated protein 1 light chain 3  $\beta$  (LC3B).

## Materials and methods

### Preparation of CPT and TFPA

TFPA was purchased from the chemical supplier Enamine, Ltd. (Kiev, Ukraine). CPT was purchased from Sigma-Aldrich (St. Louis, MO, USA). Both TFPA and CPT were dissolved in dimethyl sulfoxide (DMSO) (less than 0.1% v/v) immediately before the assays.

### Reagents

Dulbecco's modified Eagle's medium (DMEM) with high glucose, fetal bovine serum (FBS), trypan blue, DMSO and the antibiotics streptomycin and penicillin G were purchased from Gibco BRL (Gaithersburg, MD, USA). Acridine orange (AO), ribonuclease A (RNase A) and phosphate-buffered saline (PBS) were purchased from Sigma-Aldrich. Antibodies against cleaved caspase-9, cleaved caspase-3 and LC3B were purchased from Cell Signaling Technology (#9501, #9664, and #2775, respectively, San Jose, CA, USA). A LAMP2 antibody was purchased from Abcam (#ab125068, Cambridge, UK). A Cathepsin D antibody was purchased from ABclonal (#A19680, Düsseldorf, Germany). A glyceraldehyde 3-phosphate dehydrogenase (GAPDH) antibody was obtained from Santa Cruz Biotechnology (Santa Cruz, CA, USA). Both anti-mouse and anti-rabbit IgG peroxidase-conjugated secondary antibodies were purchased from Leadgene Biomedical (#20102 and #20202, respectively, Tainan, Taiwan). An Annexin V-fluorescein isothiocyanate (FITC) detection kit was purchased from Strong Biotech Co. (Taipei, Taiwan).

### Cell culture

Two human NSCLC cell lines, A549 (adenocarcinoma, *p53* wild-type) and H1299 (large cell carcinoma, *p53* null), were obtained from American Type Culture Collection (ATCC, Manassas, VA, USA). The cells were maintained in DMEM: F-12 (3:2) supplemented with 8% FBS, 2 mM glutamine, and antibiotics (100 units/ml penicillin and 100 µg/ml streptomycin) at 37 °C in a humidified atmosphere of 5% CO<sub>2</sub>.

### Assessment of proliferation inhibition

A549 and H1299 cells ( $3 \times 10^4$  cells per well in a 12-well plate) were seeded and then treated with either DMSO (vehicle) or CPT alone or in combination for 24 h and 48 h. After incubation, the cells were stained with 0.2% trypan blue in PBS and counted using a Countess™ automatic cell counter (Invitrogen, Eugene, OR, USA) [44].

### Colony formation assay

NSCLC A549 and H1299 cells ( $4 \times 10^2$ ) were seeded in 12-well plates and cultured with the indicated concentrations of CPT and TFPA alone or in combination for 11 days. The cells were fixed with 4% paraformaldehyde and

then stained with 5% Giemsa overnight. Images of each well were scanned, and the individual colony areas were counted [45].

### Assessment of apoptosis

An annexin V/PI staining assay was conducted to detect the externalization of phosphatidylserine (PS) from the cellular membrane, a hallmark of apoptosis. In brief,  $1 \times 10^5$  A549 cells were seeded into a 6-well plate and treated with the indicated concentrations of CPT (0.5 µM) and TFPA (10 µM) alone or in combination for 24 h and 48 h. Subsequently, the cells were harvested, stained with annexin V/PI (#AVK250, Strong Biotech Corporation, Taipei, Taiwan), and analyzed using an Accuri C6 flow cytometer (BD Biosciences, San Jose, CA, USA).

### Assessment of autophagy

To detect the formation of acidic vesicular organelles (AVOs), a morphological feature of autophagy, AO staining was conducted as previously described [46]. Briefly, A549 cells were seeded and incubated with the indicated concentrations of CPT (0.5 µM) and TFPA (10 µM) alone or in combination for 24 h. Subsequently, the cells were stained with AO (1 µg/mL) for 20 min and scanned with a fluorescence microscope (Olympus, Tokyo, Japan). Green AO fluorescence (510–530 nm) indicates nuclei, and red AO fluorescence (>650 nm) indicates acidic compartments.

### Immunofluorescence assay

Briefly, A549 cells were seeded into 24-well plates. After incubation, the cells were fixed with 4% paraformaldehyde and then permeabilized with 0.5% (v/v) Tween-20 in PBS. The cells were blocked with 1% (v/v) bovine serum albumin (BSA) in PBS as the blocking solution for 20 min and then incubated with the primary antibody against LC3B in blocking solution overnight at 4 °C. Subsequently, the cells were washed twice with blocking solution for 5 min and incubated with Alexa Fluor 555-conjugated goat anti-mouse immunoglobulin G (Molecular Probes, Invitrogen, Carlsbad, CA, USA). Images were analyzed by fluorescence microscopy with the TissueFAXS system (TissueGnostics GmbH, Vienna, Austria) [25].

### Confocal microscopy

Briefly,  $3 \times 10^4$  A549 cells were seeded into 24-well plates with 12-mm glass coverslips (Marienfeld Laboratory, Lauda-Königshofen, Germany) and then incubated with the indicated concentrations of CPT and TFPA alone or in combination for 24 h. After incubation, the cells were fixed with formaldehyde, permeabilized with 0.5% (v/v) Tween-20 and then incubated with blocking solution (1% BSA). The cells were incubated with an anti-LC3B

antibody and then Alexa Fluor 488-conjugated goat anti-rabbit secondary antibody (Molecular Probes, Invitrogen, Carlsbad, CA, USA). The slides were mounted with Vectashield H-1000 fluorescent mounting medium (Vector Laboratories, Burlingame, CA, USA). Immunofluorescence images were obtained with a confocal laser scanning microscope system (Olympus, Hamburg, Germany) [47].

#### Assessment of oxidative stress

The fluorescent dye DHE (MCH100111, Merck Millipore, Darmstadt, Germany) was used to evaluate the redox state of intracellular superoxide ( $O_2^{\cdot-}$ ). In brief,  $1 \times 10^5$  A549 cells were seeded in a 6-well plate and treated with 0.5  $\mu$ M CPT and 10  $\mu$ M TFPA alone or in combination for 6 h. For the assessment of ROS scavengers, the cells were pretreated with 2 mM N-acetyl-L-cysteine (NAC, A9165, Sigma-Aldrich), an ROS scavenger, for 3 h and then subjected to the indicated treatments. The cells were subsequently stained with 1  $\mu$ M DHE and incubated at 37 °C for 30 min. After incubation, the cells were harvested, washed twice with 1 ml of PBS, and resuspended in 0.2 ml of PBS. The cells were subsequently analyzed by flow cytometry with a Muse™ Cell Analyzer (Merck Millipore, Billerica, MA, USA). In the assay, we stained cells with dihydroethidium (DHE), a fluorescence dye sensitive to oxidative reactions, to quantitatively assess intracellular superoxide radicals using a flow cytometer. The areas M2 and M1 showed that all the cells were there (100%), with M2 showing the percentage of naturally occurring superoxide radicals compared to the negative control, which represented cells that did not have DHE staining.

#### Western blotting assay

Western blotting assays were conducted to detect changes in apoptosis- and autophagy-related proteins according to our previous study [48]. In brief, the harvested cells were lysed in RIPA buffer (Millipore, Temecula, CA, USA). Thirty micrograms of protein lysate was loaded on 10% SDS-polyacrylamide gel electrophoresis (SDS-PAGE) gels, and the proteins were then electrotransferred onto a polyvinylidene fluoride (PVDF) membrane (Pall Corporation, East Hills, NY, USA). The PVDF membrane was blocked with 5% nonfat milk and incubated with primary antibodies and then with the corresponding secondary antibodies. An enhanced chemiluminescence (ECL) detection kit (Advansta Corp., Menlo Park, CA, USA) was subsequently used to detect the signals of the specific proteins. The protein intensity was first normalized to the internal control, and then the relative fold changes in the protein levels were normalized by the untreated control group.

#### Zebrafish xenograft assay

A zebrafish-based tumor xenograft assay was conducted to confirm the synergistic inhibitory effect of the CPT and TFPA combination on the growth of NSCLC cells. The use and maintenance of zebrafish complied with the principles of the 3 Rs (replacement, refinement, and reduction). In brief, 48 h postfertilization (hpf) zebrafish larvae were anesthetized with 0.01% tricaine, and A549 cells were labeled with DiI, a red fluorescence dye (excitation 549 nm and emission 565 nm), and resuspended in serum-free DMEM (Life Technologies, Carlsbad, CA, USA). Fifty A549 cells were microinjected into the yolk sac of the larvae. The larvae were then incubated in distilled H<sub>2</sub>O with the CPT/TFPA combination or CPT alone for 24 h and 48 h postinjection (hpi), respectively. The masses of xenografted tumor cells were photographed using an inverted fluorescence microscope (Nikon Eclipse TE2000-U, Tokyo, Japan).

#### Statistical analysis

All data are presented as the means  $\pm$  standard deviations (SDs) of three independent experiments. The significance of the difference between the cells treated with the combination of CPT with TFPA and the cells treated with CPT alone was analyzed by one-way analysis of variance (ANOVA).  $p < 0.05$  was considered to indicate statistical significance.

## Results

#### Effect of TFPA on CPT-induced inhibition of NSCLC cell proliferation

The trypan blue exclusion assay revealed compelling evidence showing synergy when CPT and TFPA were combined, leading to marked inhibition of cellular proliferation in both NSCLC cell lines (Fig. 1A and B). Notably, this synergy extended to the suppression of clonogenicity, as illustrated in Fig. 1C and D, underlining the potent antiproliferative potential of this combination therapy. These results emphasize the promising therapeutic implications of concurrent CPT and TFPA administration in the context of NSCLC treatment, which warrants further investigation.

#### Effect of TFPA on CPT-induced NSCLC cell death

To examine whether the combination of CPT and TFPA synergistically inhibits NSCLC cell proliferation by inducing apoptosis, apoptotic cells were detected using an annexin V/PI dual staining assay. Annexin V-positive/PI-negative and annexin V-positive/PI-positive cells were considered early- and late-apoptosis populations, respectively. As shown in Fig. 2A and B, treatment with CPT alone moderately induced apoptosis in A549 cells at both 24 h and 48 h, and TFPA alone did not induce significant apoptosis in A549 cells. In comparison with treatment

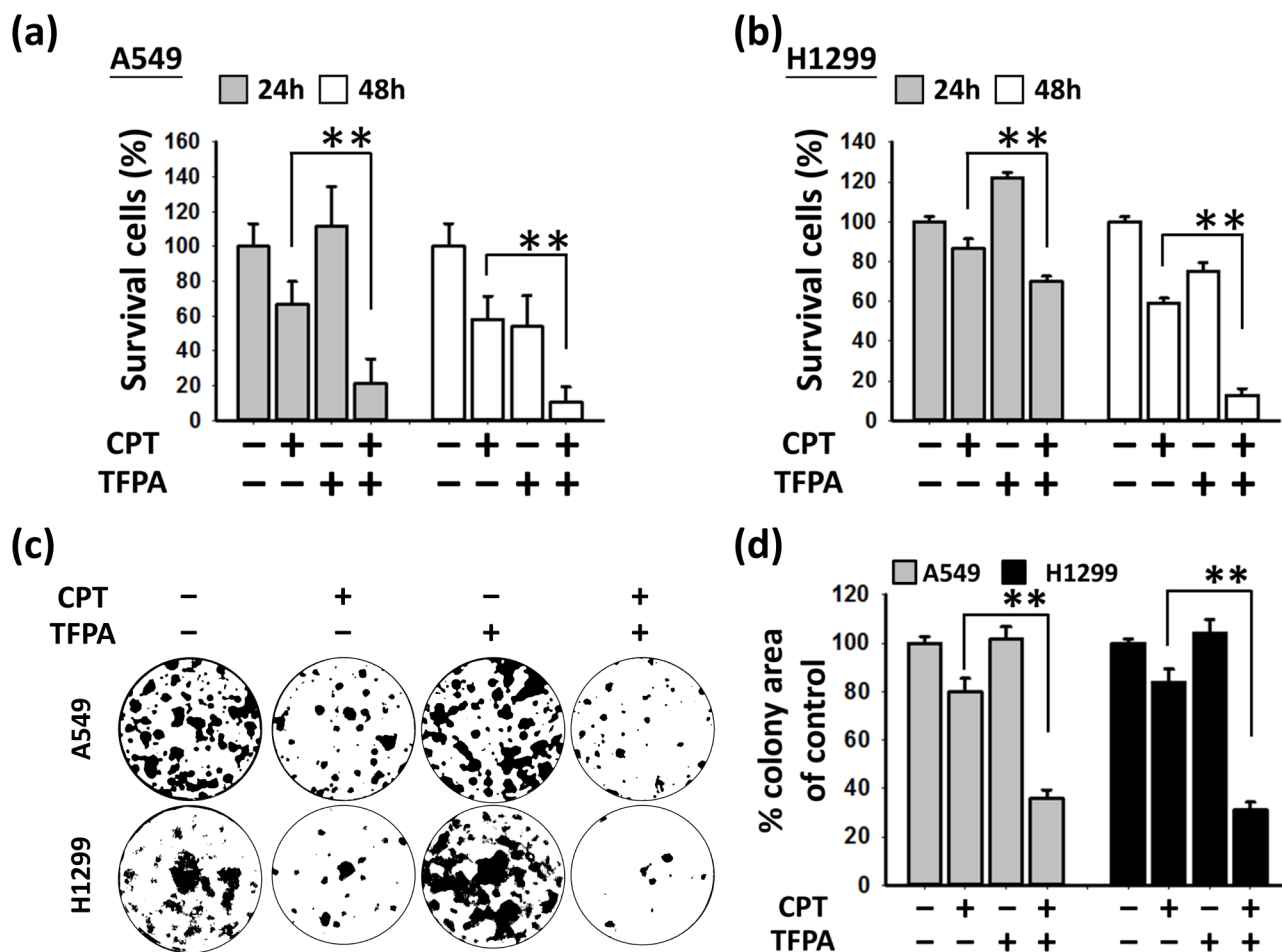


**Fig. 1** Effects of the combination of CPT and TFPA on the cell proliferation and survival of NSCLC cell lines. H1299 cells were treated with the indicated doses of CPT and TFPA alone or in combination for 48 h. A trypan blue exclusion assay was performed to measure the proliferation rate of H1299 cells. **A** and **B** NSCLC cells A549 and H1299 were treated with 0.5  $\mu$ M CPT and 10  $\mu$ M TFPA alone or in combination for 24 h and 48 h. The cell survival rate was determined (\*\* $p < 0.001$ ). **C** Results of a colony formation assay for evaluating the effect of the combination of 0.5  $\mu$ M CPT and 10  $\mu$ M TFPA on the long-term proliferation of NSCLC cells. **D** Quantification of the results in **C** (\*\* $p < 0.001$ )

with CPT or TFPA alone, the combination of CPT and TFPA synergistically induced the apoptosis of A549 cells. Similarly, Western blot results showed increased cleavage of caspase-9 and caspase-3, suggesting that cotreatment with TFPA could further increase the levels of apoptosis-related proteins in both A549 (Fig. 2C and D) and H1299 cells (Additional file 1).

#### Autophagic induction and maturation of A549 cells after CPT/TFPA cotreatment

Autophagic cell death induced by anticancer compounds is usually accompanied by the formation of large-scale autophagic vacuolization in the cytoplasm of cells [49, 50]. As shown in Fig. 3A, we found that CPT/TFPA cotreatment induced the formation of vesicles in A549 cells after incubation for 24 h, suggesting that autophagy was induced in A549 cells by cotreatment with CPT and TFPA. In this study, we used AO, a nucleic acid-selective fluorescent cationic dye, to detect AVOs (Fig. 3B).

Furthermore, the formation of LC3B puncta is the hallmark of the maturation of autophagosomes [51], and the results showed that CPT/TFPA cotreatment markedly increased the formation of LC3B puncta in A549 cells (Fig. 3C and D).

#### CPT/TFPA cotreatment impairs both autolysosome formation and lysosomal function

A previous study showed that impairing autophagy contributes to the death of cancer cells [52]. Therefore, we further investigated whether CPT/TFPA cotreatment induced A549 cell death by modulating autophagy. As shown in Fig. 4A and B, Western blotting showed that CPT/TFPA cotreatment induced the accumulation of LC3B-II, a marker of autophagosomes, and LAMP2, a marker of lysosomes, in A549 cells to a greater extent than that observed with CPT treatment alone. Additionally, the expression of SQSTM1/p62, an important substrate of autophagosome enzymes [53], and cathepsin

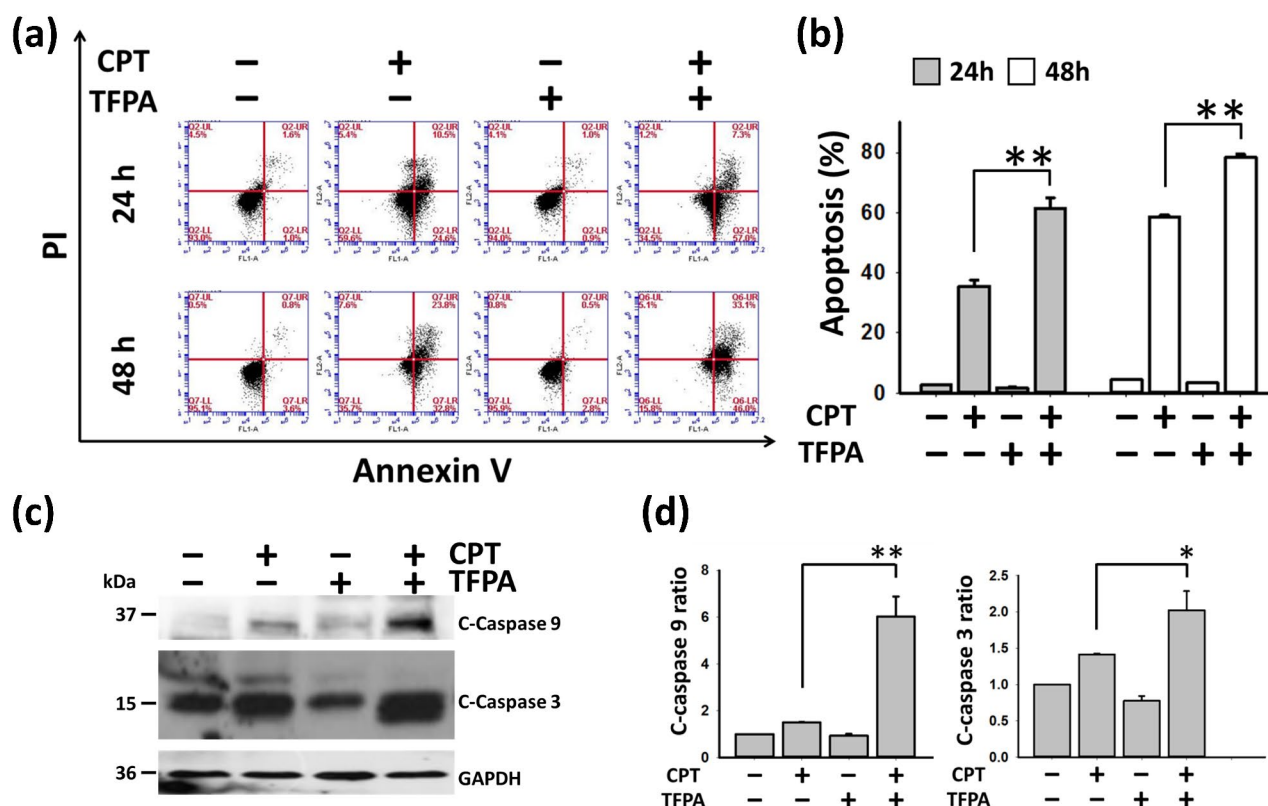


**Fig. 2** Cotreatment with CPT and TFPA synergistically promotes the apoptosis of A549 cells. The cells were treated with the indicated concentrations of CPT and TFPA alone or in combination for 24 h and 48 h. **A** Apoptosis was assessed by annexin V/PI staining and flow cytometry. **B** Quantification of the results in **A** (\*\* $p < 0.001$ ). **C** Western blot assays were performed to analyze the changes in the expression of apoptosis-related proteins, including C-caspase-9 and C-caspase 3. C-caspase-9 indicates cleaved caspase-9; C-caspase 3 indicates cleaved caspase 3. GAPDH was used as an internal control to ensure equal loading. **D** Quantification of the results in **C**

D, a lysosomal enzyme [54], was decreased in A549 cells after cotreatment with CPT and TFPA compared with CPT alone (Fig. 4A). Furthermore, cotreatment with CPT and TFPA induced localization of LC3 primarily in the nuclei, whereas a marked decrease in cytoplasmic LC3 was observed (Fig. 4C). These results suggested that CPT/TFPA cotreatment impaired the translocation of LC3 from nuclei to the cytoplasm, which may block the fusion of autophagosomes and lysosomes in the cytoplasm, and led to increased perinuclear localization of LC3 compared with CPT alone, whereas CPT/TFPA cotreatment appeared to induce accumulation of nuclear LC3.

#### TFPA enhances CPT-induced ROS production in NSCLC cells

A previous study found that the regulation of endogenous ROS is highly correlated with the fusion of autophagosomes and lysosomes during the autophagy process [55]. Therefore, we further examined whether CPT/TFPA cotreatment synergistically increases the ROS levels in A549 cells. Dihydroethidium (DHE), a superoxide ( $O_2^-$ ) indicator, was used to detect the intracellular levels of ROS in cells [56]. A flow cytometry-based analysis

showed that the level of endogenous ROS in A549 cells cotreated with CPT and TFPA was higher than that in cells treated with CPT alone for 6 h (Fig. 5A and B), suggesting that TFPA synergistically enhances CPT-induced endogenous ROS accumulation in A549 cells. In contrast, NAC, an ROS scavenger, was used to scavenge ROS [57]. Next, we examined whether NAC reduces CPT/TFPA cotreatment-induced ROS production in A549 cells. As described in Fig. 5, ROS scavenging by NAC significantly reduced CPT/TFPA cotreatment-induced ROS production in A549 cells. These results suggest that CPT/TFPA cotreatment increases the endogenous ROS levels in A549 cells.

#### ROS scavenger treatment attenuates CPT/TFPA cotreatment-induced cell death in NSCLC cells

We examined whether ROS play a role in the CPT/TFPA combination-induced apoptosis of NSCLC cells. As shown in Fig. 6A and B, NAC, an ROS scavenger, moderately reduced CPT/TFPA cotreatment-induced apoptosis of A549 cells, suggesting that TFPA sensitizes A549 cells toward CPT-induced apoptosis by promoting ROS generation. Furthermore, we evaluated the effect of

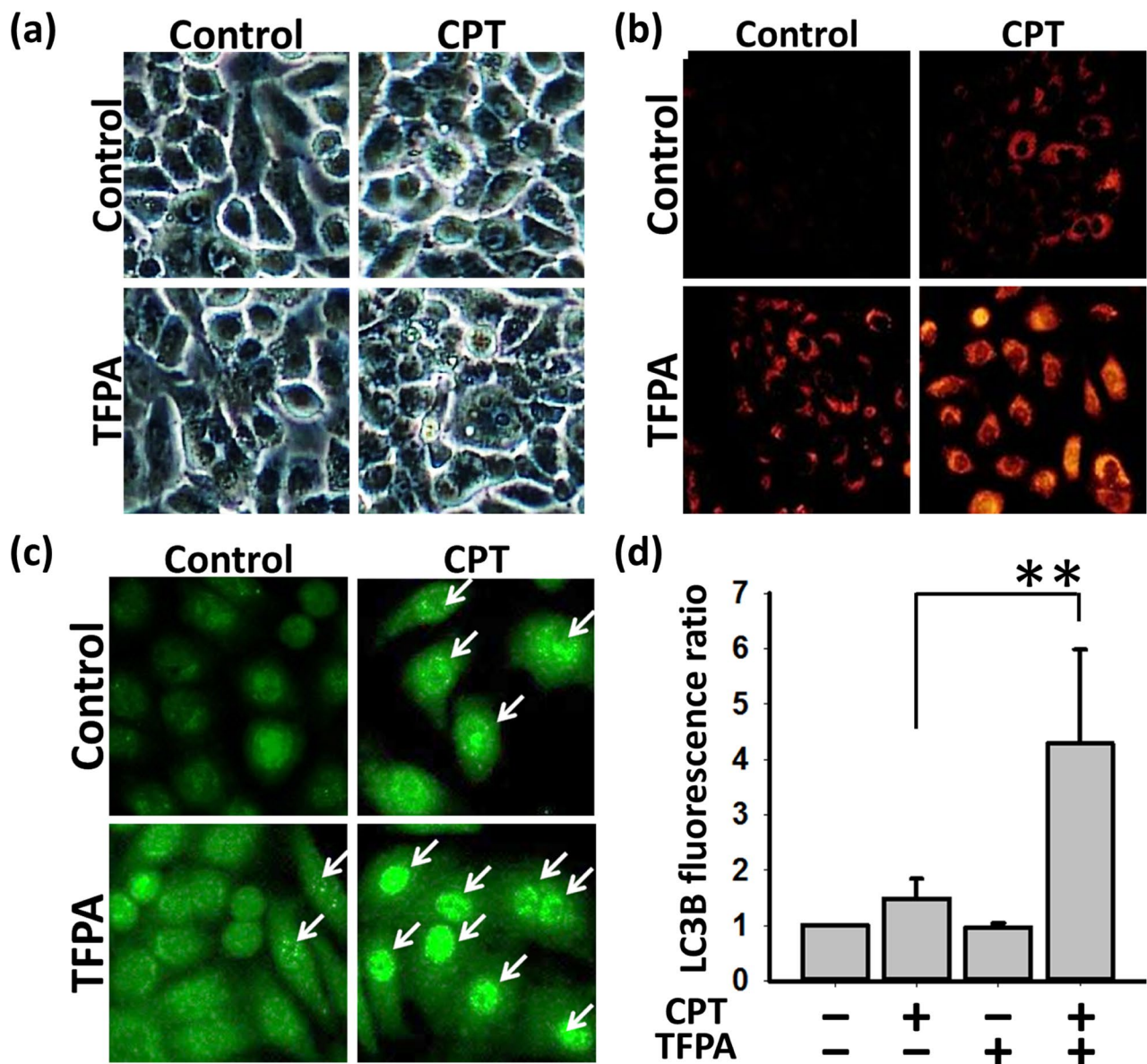


**Fig. 3** The combination of CPT and TFPA increases autophagy in NSCLC cells. A549 cells were treated with the indicated concentrations of CPT (0.5  $\mu$ M) and TFPA (10  $\mu$ M) alone or in combination for 24 h. **A** The combination of TFPA and CPT increased the formation of vesicles, which were observed by phase-contrast microscopy. **B** Detection of AVOs, the hallmark of autophagy, induced by the combination of CPT and TFPA using AO staining. **C** Formation of LC3B puncta in A549 cells after cotreatment with CPT and TFPA (the white arrows indicate the formation of LC3B puncta, a marker of autophagosomes). **D** Quantification of the results in **C** (\*\* $p < 0.001$ ). Magnification: 100x

ROS on CPT/TFPA cotreatment-induced expression of LC3B-II, SQSTM1/p62 and LAMP2, a lysosome-related protein, in A549 cells by Western blotting. As shown in Fig. 6C and D, Western blotting showed that NAC rescued the protein expression of LC3B-II, SQSTM1/p62 and LAMP2 in A549 cells, suggesting that CPT/TFPA cotreatment-induced ROS production blocks the fusion of autophagosomes with lysosomes.

#### CPT/TFPA cotreatment inhibits the proliferation of NSCLC cells in a zebrafish xenograft model

We further examined whether cotreatment with CPT and TFPA synergistically inhibits the proliferation of A549 cells in zebrafish [58]. Cells were prestained with DiI (red fluorescent dye) and implanted into the yolk sac of zebrafish larvae for 24 and 48 h, and the larvae were then incubated with CPT and TFPA alone or in combination. Consistent with the in vitro findings, the zebrafish xenograft assay demonstrated that TFPA cotreatment

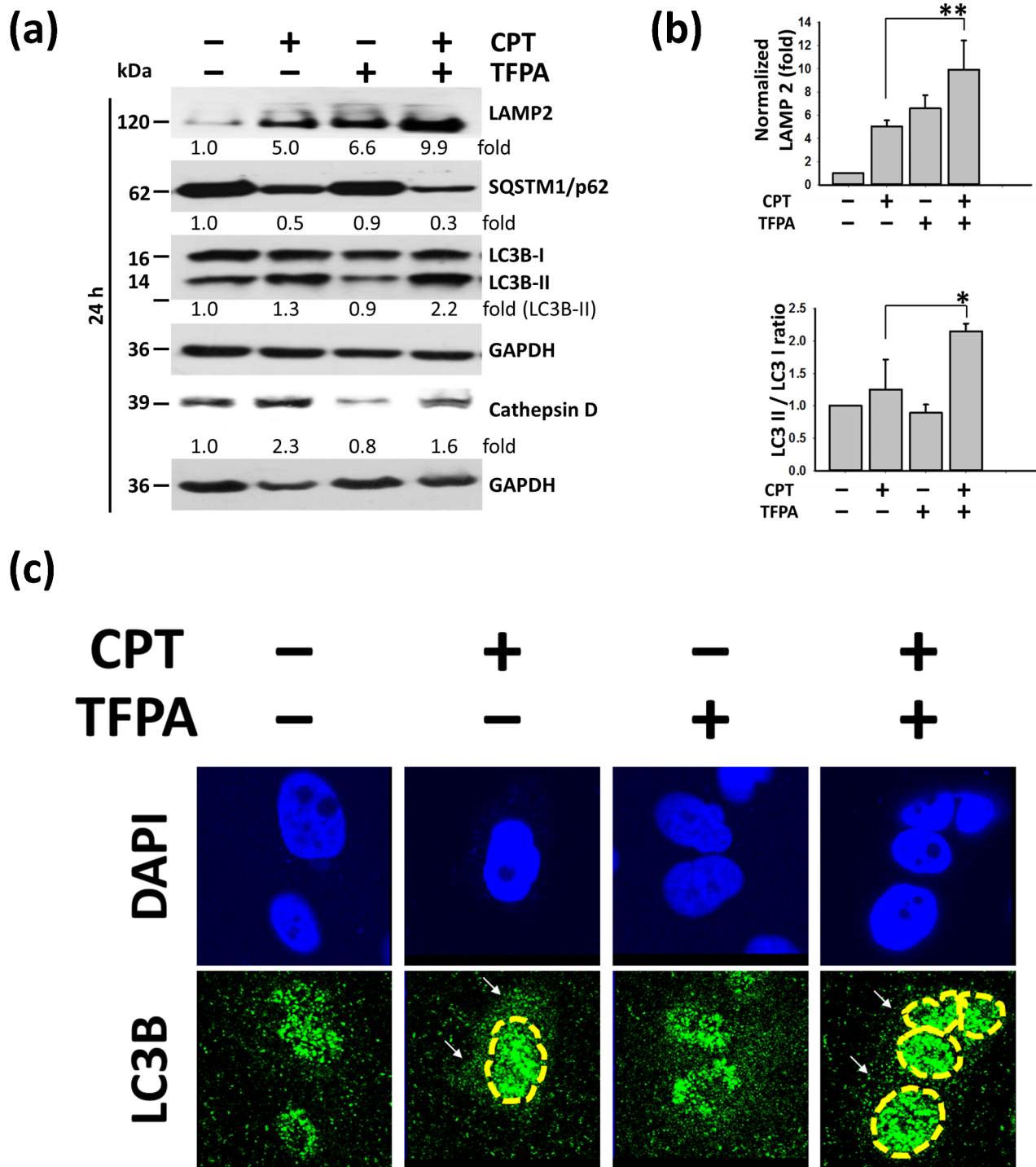


**Fig. 4** CPT/TFPA cotreatment induces nuclear retention of LC3B and blocks the fusion of autophagosomes with lysosomes in A549 cells. The cells were treated with CPT (0.5  $\mu$ M) and TFPA (10  $\mu$ M) alone or in combination for 24 h. **A** Western blot analysis showed that CPT/TFPA cotreatment increased the protein levels of LC3B-II and LAMP2 but decreased the protein levels of SQSTM1/p62 and cathepsin D. The protein intensity was first normalized to the internal control GAPDH, and then the relative fold changes in the protein levels were normalized by the untreated control group. **B** Quantification of the results in **A** ( $*p < 0.05$ ;  $**p < 0.001$ ). **C** Analysis of the localization of LC3B in A549 cells using a confocal microscopy-based immunofluorescence assay (the yellow dotted lines indicate the region of nuclei). Magnification: 1000 x. The dotted line (yellow line) indicates the nuclear regions. DAPI was used as a nuclear marker (Blue fluorescence); LC3B was used as a marker of autophagosomes (Green fluorescence)

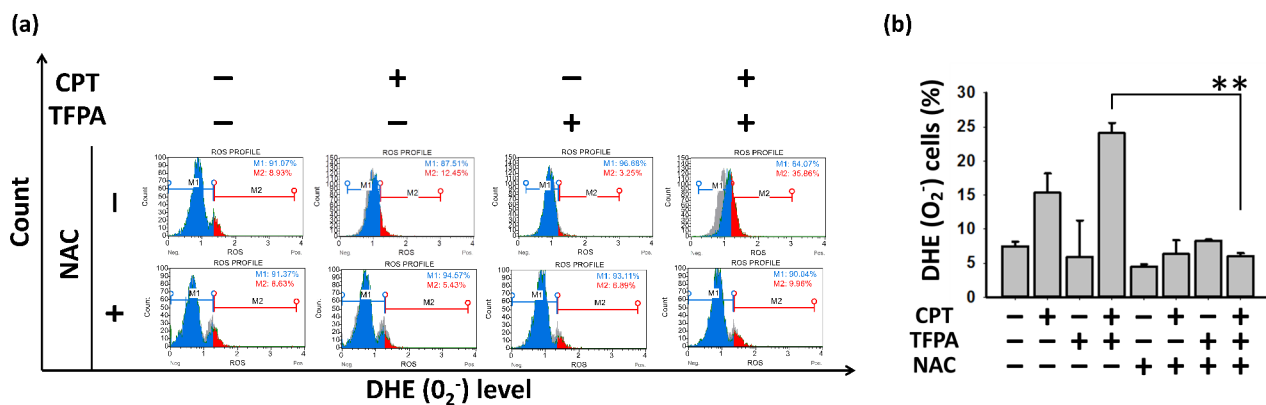


**Fig. 5** Cotreatment with CPT and TFPA enhances ROS production in A549 cells. The cells were treated with CPT (0.5 μM) and TFPA (10 μM) alone or in combination for 6 h, respectively. **A** The production of endogenous ROS was determined using a flow cytometer-based DHE staining assay. Pretreatment with NAC as an ROS scavenger. **B** Quantification of the results in **A** (\*\**p* < 0.001)

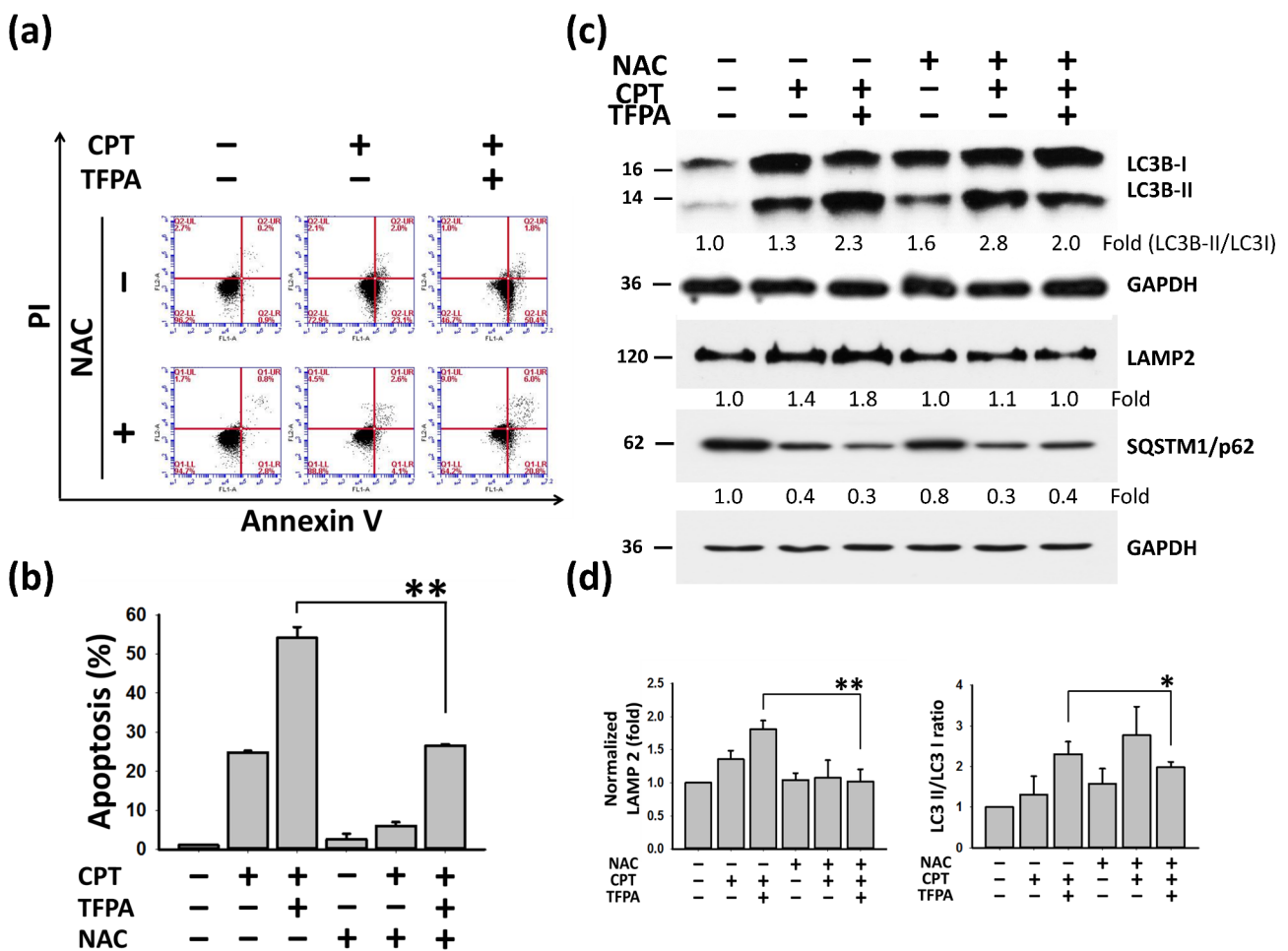


**Fig. 6** Role of ROS in TFPA/CPT-induced apoptosis and autophagy in NSCLC cells. A549 cells were pretreated with 2 mM NAC for 3 h before CPT/TFPA cotreatment. **A** Annexin V/PI dual staining was performed to examine the apoptotic cell population. **B** Relative levels of apoptotic cells in treated groups with and without pretreatment with NAC (\*\**p* < 0.001). **C** Expression of the autophagosome-related protein LC3B and lysosome-related protein LAMP2. **D** Quantification of the Western blot results. The vehicle group was used as the normalization control (\**p* < 0.05; \*\**p* < 0.001)

effectively suppressed the growth of implanted A549 cells (Fig. 7A and B), validating that TFPA treatment enhances the inhibitory effect of CPT on the growth of NSCLC cells both in vitro and in vivo.

## Discussion

Although chemotherapy is primarily used to treat NSCLC patients, most NSCLCs acquire resistance to chemotherapy [19, 59]. For instance, topoisomerase inhibitors, such as topotecan, are widely used in the treatment of lung cancer patients and as second-line therapy [60]. However, the 5-year recurrence rate of NSCLC patients after topotecan treatment could reach 50% [19]. Fortunately, several studies have found that aniline-containing compounds may contribute to enhancing radiotherapy or chemotherapy-based treatment strategies for lung cancer. For example, 4-(2-cyclohexylethoxy) aniline (IM3829) synergistically increases the radiation-induced apoptosis of H1299 cells [38]. Additionally, acetaminophen, an aniline-containing compound, synergistically increases both cisplatin- and paclitaxel-induced antiproliferation of human ovarian cancer SKOV3 cells [61].

In this study, we found that both the trypan blue exclusion assay and colony formation assay showed that the CPT/TFPA combination inhibited the proliferation of NSCLC cells (Fig. 1). Therefore, these results indicate the effects of TFPA on CPT-induced inhibition of NSCLC cell proliferation. Increased viability was observed with TFPA treatment alone compared to the control. Further statistical analysis showed that the difference was only significant in H1299 cells, as shown in Fig. 1B ( $p < 0.001$ ), but not significantly different in A549 cells in Fig. 1A ( $p = 0.91$ ). Based on our results, we suggested that this hormesis-like response may be due to cellular

overcompensation to the low-dose toxin exposure. As reported in the literature, hormesis manifests as a biphasic dose response with increased stimulatory or beneficial effects at low doses and inhibitory or toxic effects at high doses [62]. The exact molecular mechanisms remain to be fully elucidated but may involve pathway overactivation. While this issue should be further investigated, the central finding is that TFPA significantly potentiates the antiproliferative and cytotoxic activity of CPT in NSCLC cells, consistent with the overall conclusions regarding the therapeutic potential of this combination.

Two major signaling cascades of apoptosis are the intrinsic/mitochondrion-mediated apoptosis pathway and the extrinsic/death receptor-mediated apoptosis pathway [63]. Our results showed that TFPA increased the apoptosis rate of A549 cells by approximately 20% compared with that found with CPT treatment alone (Fig. 2A and B). Compared with CPT alone, the CPT/TFPA combination increased the proteolytic activation of the initiator caspase of the mitochondria-mediated apoptosis pathway, caspase-9, and the effector caspase-3, which are hallmarks of apoptosis, in A549 cells (Fig. 2C and D).

In addition to apoptosis, there are several known non-apoptotic mechanisms that contribute to cell death, such as necrosis and autophagy [64, 65]. Autophagy is a conserved lysosome-mediated mechanism by which cells can degrade various macromolecules and organelles and therefore plays a prosurvival role in response to stresses such as starvation in healthy cells [66]. Autophagy involves the sequestration of the cytoplasm and damaged organelles within double-membrane autophagosomes, where the organelles are eventually degraded by lysosomal hydrolases [67]. Additionally, the process

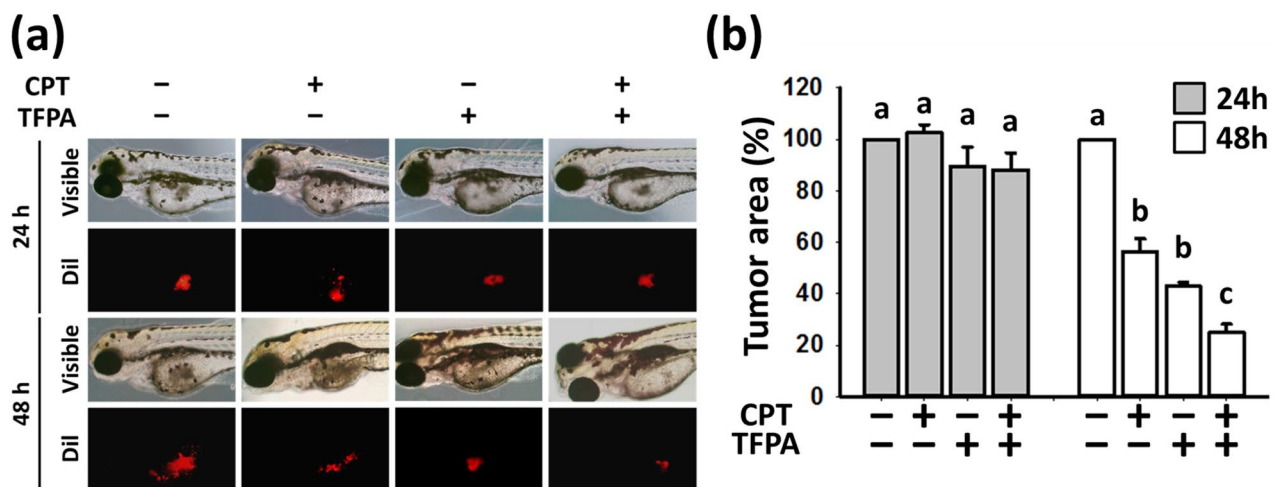


**Fig. 7** Results of the in vivo zebrafish xenograft model. A549 cells were labeled with the red fluorescence dye Dil and injected into the yolk sac of zebrafish larvae. Subsequently, the larvae were incubated with the indicated treatments for zebrafish for 24 h and 48 h, respectively. **A** The intensity of red fluorescence indicates the mass size of the xenograft tumor.  $N = 15$ . **B** Quantitative results of **A** ( $^a p > 0.05$ ,  $^b p < 0.05$ ,  $^c p < 0.001$ ). Magnification: 100x

of autophagy includes five stages: initiation, elongation, autophagosome maturation, fusion of lysosomes and autophagosomes, and final degradation of damaged organelles or macromolecules [27].

Anticancer drug-induced autophagy is thought to contribute to cell survival and therefore promotes the chemoresistance of cancer cells [68–70]. Zhang's work showed that autophagy delays the CPT-induced cell death of human colon cancer HCT116 cells [22]. Furthermore, recent studies have found that the *disruption of autophagy significantly increases the chemotherapeutic agent-induced cell death of cancer cells* [40, 71, 72]. For instance, chloroquine (CQ), an autophagy inhibitor, promotes the topotecan-induced death of A549 cells by impairing the formation of autolysosomes [41]. Similarly, CQ has been shown to sensitize A549 cells to treatment with BEZ235, a PI3K/mTOR inhibitor [73]. Accordingly, the abovementioned studies suggest that impairment of the autophagy process could be a strategy for lung cancer treatment [52]. Moreover, anticancer drug-induced cell death may be accompanied by the accumulation of cytoplasmic vacuoles rather than by the formation of apoptotic bodies [50]. Trabbic et al. found that 2-indolyl substituted pyridinylpropanones, indole-based chalcones, induce death of glioblastoma cells U251 by regulating massive cytoplasmic vacuolization, a hallmark of autophagic cell death [74]. The modulation of mitochondrial apoptosis and autophagic flux by drug combinations is considered to be a promising strategy for sensitizing cancer cells. For example, Hajiahmadi reported that the combination of simvastatin (Simva), cholesterol-lowering medications, and acetylshikonin increased temozolomide-induced cell death in the glioblastoma multiforme (GBM) cell lines U87 and U251 by modulating autophagic flux [75]. Our findings are consistent with recent studies exploring combination therapies for GBM, such as the work by Hajiahmadi S et al. demonstrating increased apoptosis and potential involvement of mitochondrial dysfunction [75]. While our study focused on impairing autophagy with aniline TFPA to increase CPT-induced cell death, further confirmation of the role of autophagy is required. Therefore, we examined whether autophagic cell death contributes to CPT/TFPA-induced death. We found that the CPT/TFPA combination induced accumulation of cytoplasmic vacuoles (Fig. 3A) and enhanced the formation of AVOs (Fig. 3B). Furthermore, the CPT/TFPA combination increased LC3 puncta, suggesting autophagy induction (Fig. 3C and D).

We further found that TFPA increased the CPT-induced accumulation of both LC3B-II, a marker of autophagosomes, and LAMP2, a marker of lysosomes (Fig. 4A and B). In contrast, the expression of cathepsin D, a lysosome-associated enzyme [76], and SQSTM1/p62, a vital substrate for lysosomal degradation [77],

was markedly decreased by CPT/TFPA cotreatment in A549 cells (Fig. 4A). Recently, Li's work suggested that the inhibition of cathepsin D enhances dysfunction of the autophagy-lysosome pathway [78], suggesting that the CPT/TFPA combination may impair autophagy in NSCLC cells.

Interestingly, our results showed that the nuclear retention of LC3B was increased by the CPT/TFPA combination in A549 cells (Fig. 3C). Under healthy or nutrient-abundant conditions, LC3 is acetylated and distributed in both the nucleus and cytoplasm. However, under nutrient depletion or other stress conditions, LC3 is deacetylated and then translocated from the nucleus to the cytosol. LC3 redistribution promotes the maturation of autophagosomes [79]. Recent studies have suggested that arresting or blocking the process of autophagy could be a promising strategy for enhancing the cytotoxicity of anticancer drugs. Chen's work found that graphene oxide, a nanomaterial, in combination with cisplatin increases cytotoxicity in CT26 colorectal cancer by blocking the redistribution of LC3 from the nucleus to the cytoplasm [80], suggesting that the nuclear retention of LC3 blocks the maturation of autophagosomes, a critical stage of autophagy.

During the process of autophagy, the fusion of lysosomes and autophagosomes is the key step in autolysosome formation, and lysosomal degradation ensures the progression of autophagy [81]. Insufficient activity or downregulated expression of the lysosomal enzyme cathepsin D could cause dysfunction of lysosomal degradation [72, 82], which may cause autolysosome dysfunction. Accordingly, our present results showed that TFPA might not only impair lysosomal degradation by downregulating the lysosomal enzyme cathepsin D but also prevent autophagosome maturation by changing the distribution of LC3.

The involvement of ROS in activating autophagy was reported previously [83, 84]. Chen et al. proposed that superoxide ( $O_2^-$ ), one of the most common free radicals, plays a role in regulating autophagy [85]. In contrast, increased levels of ROS can sensitize cancer cells to chemotherapy [86]. For example, Ma K et al. found that cinobufagin, which was isolated from *Chan Su*, increased the autophagy-mediated cell death of osteosarcoma U2OS through increased ROS production [87]. Similarly, psoralidin, isolated from *Psoralea corylifolia* L., induced cell death in NSCLC by blocking autophagosome-lysosome fusion [55]. Our results showed that TFPA synergistically enhanced CPT-induced ROS in A549 cells, and pretreatment with NAC, an ROS scavenger, partially reduced ROS accumulation and apoptosis after CPT/TFPA cotreatment (Figs. 5 and 6), suggesting that ROS play a promoting role in CPT/TFPA-induced

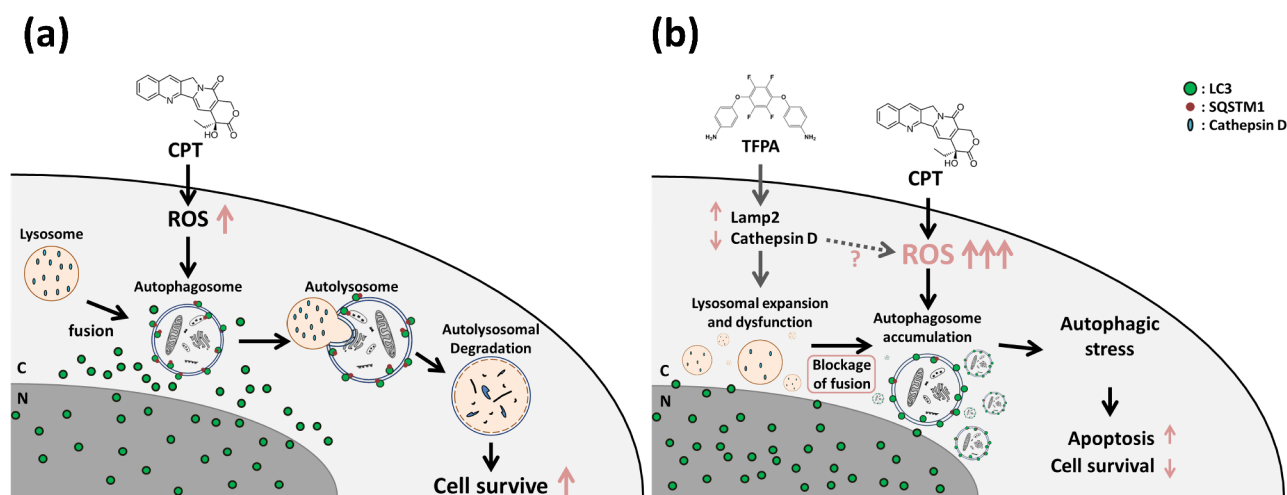


**Fig. 8** Potential regulatory mechanism of TFPA in CPT-mediated cell death. When lung cancer cells are treated with CPT alone **A**, it induces moderate ROS production, triggering protective autophagy that promotes cellular survival and contributes to CPT resistance in NSCLC cells. However, TFPA increases CPT-induced ROS levels **B**, resulting in significant nuclear retention of LC3 and a reduction in cytoplasmic LC3 levels. This process impairs autophagy, hindering the fusion of autophagosomes and lysosomes in the cytoplasm, ultimately inducing autophagic stress and leading to cell death of NSCLC cells

autophagosome accumulation and lysosomal expansion in A549 cells.

Zebrafish (*Danio rerio*) are small, and their embryos are transparent and undergo rapid development; therefore, they are an ideal model organism for disease and drug discovery [88]. We used a zebrafish xenograft assay to validate the inhibitory effects of CPT/TFPA cotreatment on NSCLC cells in vivo. Consistent with the in vivo results, the CPT/TFPA cotreatment synergistically inhibited the cell growth of A549 cells compared with that observed with CPT treatment alone (Fig. 7).

Based on our observations, the accumulation of autophagosomes (increased LC3B-II) and lysosomal expansion (increased LAMP2), along with reduced levels of cathepsin D and p62, indicates impaired lysosomal degradation [89]. Remarkably, we also noted increased nuclear retention of LC3B, suggesting a potential interference with autophagosome maturation. Therefore, our findings suggest that CPT/TFPA treatment impedes autophagy in NSCLC cells, particularly by obstructing autophagosome-lysosome fusion and subsequent autolysosomal degradation. The interplay between ROS and autophagy is intricate and extensively studied. ROS can serve as signaling molecules that induce autophagy, thereby mitigating oxidative stress through damaged organelle and protein degradation. However, excessive ROS could impair autophagy and lead to cell death [90].

Given that CPT and TFPA are known to elevate ROS production, the observed autophagic impairment may partly be due to increased ROS levels disrupting autophagic processes. Our study suggests a potential role for ROS in CPT/TFPA-induced autophagy impairment, which could be further explored using ROS scavengers such as

NAC, which reduces intracellular ROS levels. Assessing its impact on autophagy in the context of CPT/TFPA treatment could determine whether ROS modulation can alleviate autophagic stress and increase cell viability.

Our study showed that the CPT/TFPA combination induced cell death in NSCLC by impairing autophagy, employing advanced autophagic flux assays, such as those using lysosomal inhibitors, or the tandem fluorescent reporter system (GFP-LC3-RFP/mCherry-LC3ΔG), as proposed by Kaizuka et al. [91] and Tanaka et al. [92]; therefore, the above assessments, which provide direct evidence of how the CPT/TFPA combination disturbs autophagy at different stages in NSCLC cells, will be included in our future study.

## Conclusions

Our present results suggest that TFPA enhances CPT-induced proliferation inhibition and cell death in NSCLC cells. CPT/TFPA cotreatment blocked the fusion of autophagosomes and lysosomes, possibly through the retention of nuclear LC3B and the modulation of lysosome activity, causing autophagy impairment. Furthermore, cotreatment with CPT and TFPA increased the ROS levels and reduced the apoptotic threshold, sensitizing NSCLC toward cell death (Fig. 8). The aniline derivative TFPA could be a promising sensitizer to CPT-based treatment for lung cancer in the future.

## Abbreviations

ANOVA	Analysis of variance
AO	Acridine orange
ATCC	American Type Culture Collection
AVOs	Acidic vesicular organelles
BSA	Bovine serum albumin
CPT	Camptothecin

CQ	Chloroquine
DHE	Dihydroethidium
DMEM	Dulbecco's modified Eagle's medium
DMSO	Dimethyl sulfoxide
FBS	Fetal bovine serum
FITC	Fluorescein isothiocyanate
GAPDH	Glyceraldehyde 3-phosphate dehydrogenase
hpf	Hours postfertilization
hpi	Hours postinjection
LC3B	Microtubule-associated protein 1 light chain 3β
3-MA	3-methyladenine
NAC	N-acetyl-L-cysteine
NSCLC	Non-small cell lung cancer
PBS	Phosphate-buffered saline
PS	Phosphatidylserine
PVDF	Polyvinylidene fluoride
RNase A	Ribonuclease A
ROS	Reactive oxygen species
SD	Standard deviation
SDS–PAGE	SDS-polyacrylamide gel electrophoresis
TFPA	4-[4-(4-aminophenoxy)-2,3,5,6-tetrafluorophenoxy] aniline

## Supplementary Information

The online version contains supplementary material available at <https://doi.org/10.1186/s12935-025-03657-6>.

Additional file 1: Synergistic effect of CPT/TFPA cotreatment on the apoptosis of H1299 cells. The cells were treated with the indicated concentrations of CPT and TFPA alone or in combination for 24 h and 48 h. **A** Apoptosis assessment by annexin V/PI staining. **B** Quantitative analysis of the results in **A** (\* $p < 0.05$  and \*\* $p < 0.001$ ). **C** Expression of proapoptotic proteins. C-caspase-9 indicates cleaved caspase-9; C-caspase 3 indicates cleaved caspase 3. GAPDH was used as an internal control

## Acknowledgements

We are grateful to the Center for Research Resources and Development (Kaohsiung Medical University, Kaohsiung, Taiwan) for providing instrument support (flow cytometry and confocal laser scanning microscopy).

## Author contributions

Experimental designs: HLC and CCC; reagents and materials: ILL, YTC, WTC, WCC, CYW, SJC and CWS; bioassays: HLC and AY; manuscript preparation and writing: HLC, CCC and PFL.

## Funding

We thank the following institutions for providing financial support: National Science and Technology Council, Taiwan (grant number NSTC 113-2320-B-037-029-MY3); NSYSU-KMU joint grants (grant numbers NSYSUKMU111-P11, NSYSU-KMU-112-P24, NSYSUKMU113-P04 and NSYSUKMU114-P02); NKUST-KMU joint grant (grant number 114KK003); the Kaohsiung Medical University Research Center, Taiwan (grant number KMU-TC113A04); the Kaohsiung Medical University, Taiwan (grant number KMU-M111024); and the Kaohsiung Medical University Hospital (KMUH) (grant numbers KMUH108-6R38 and KMUH113-3M61).

## Data availability

The datasets supporting the conclusions of this article are included within the article.

## Declarations

### Ethics approval and consent to participate

Not applicable.

### Consent for publication

Not applicable.

### Competing interests

The authors declare no competing interests.

## Author details

<sup>1</sup>Department of Biotechnology, Kaohsiung Medical University, Kaohsiung 807, Taiwan

<sup>2</sup>Department of Medical Laboratory Science and Biotechnology, Kaohsiung Medical University, Kaohsiung 807, Taiwan

<sup>3</sup>Department of Laboratory Medicine, Kaohsiung Medical University Hospital, Kaohsiung 807, Taiwan

<sup>4</sup>Department of Life Sciences, Institute of Genome Sciences, National Yang Ming Chiao Tung University, Taipei 112, Taiwan

<sup>5</sup>Division of General and Digestive Surgery, Department of Surgery, Kaohsiung Medical University Hospital, Kaohsiung 807, Taiwan

<sup>6</sup>Department of Surgery, School of Medicine, College of Medicine, Kaohsiung Medical University, Kaohsiung 807, Taiwan

<sup>7</sup>Center for Cancer Research, Kaohsiung Medical University, Kaohsiung 807, Taiwan

<sup>8</sup>Department of Biological Sciences, National Sun Yat-sen University, Kaohsiung 804, Taiwan

<sup>9</sup>Department of Biochemistry, College of Medicine, Kaohsiung Medical University, Kaohsiung 807, Taiwan

<sup>10</sup>Institute of Biopharmaceutical Sciences, National Sun Yat-sen University, Kaohsiung 804, Taiwan

<sup>11</sup>The Graduate Institute of Medicine, Kaohsiung Medical University, Kaohsiung 807, Taiwan

<sup>12</sup>Department of Medical Research, Kaohsiung Medical University Hospital, Kaohsiung 807, Taiwan

<sup>13</sup>Department of Biomedical Science and Environmental Biology, Kaohsiung Medical University, Kaohsiung 807, Taiwan

Received: 18 October 2023 / Accepted: 21 January 2025

Published online: 07 March 2025

## References

- Pakzad R, Mohammadian-Hafshejani A, Ghoncheh M, Pakzad I, Salehiniya H. The incidence and mortality of lung cancer and their relationship to development in Asia. *Transl Lung Cancer Res.* 2015;4(6):763–74.
- Siegel RL, Miller KD, Fuchs HE, Jemal A. Cancer statistics, 2022. *CA Cancer J Clin.* 2022;72(1):7–33.
- Kuribayashi K, Funaguchi N, Nakano T. Chemotherapy for advanced non-small cell lung cancer with a focus on squamous cell carcinoma. *J Cancer Res Ther.* 2016;12(2):528.
- Arnold SM, Chansky K, Baggstrom MQ, Thompson MA, Sanborn RE, Villano J, Waqar SN, Hamm JT, Leggas M, Willis M, et al. Phase II trial of carfilzomib and irinotecan in relapsed small cell lung cancer (NCT01941316). *J Clin Oncol.* 2019;37(15suppl):8513–3.
- Ernani V, Jahan R, Smith LM, Marr AS, Kimbrough SE, Kos ME, Tijerina J, Pivovar S, Lakshmanan I, Ketcham M. A phase I study of weekly doxorubicin and oral topotecan for patients with relapsed or refractory small cell lung cancer (SCLC): a Fred and Pamela Buffet Cancer Center Clinical Trials Network study. *Cancer Treat Res Commun.* 2020;22:100162.
- Fennell DA, Summers Y, Cadranel J, Benepal T, Christoph DC, Lal R, Das M, Maxwell F, Visseren-Grul C, Ferry D. Cisplatin in the modern era: the backbone of first-line chemotherapy for non-small cell lung cancer. *Cancer Treat Rev.* 2016;44:42–50.
- Rotow J, Bivona TG. Understanding and targeting resistance mechanisms in NSCLC. *Nat Rev Cancer.* 2017;17(11):637.
- Ashrafzadeh M, Zarrabi A, Hushmandi K, Hashemi F, Moghadam ER, Owrang M, Hashemi F, Makvandi P, Goharizi MASB, Najafi M, et al. Lung cancer cells and their sensitivity/resistance to cisplatin chemotherapy: role of microRNAs and upstream mediators. *Cell Signal.* 2021;78:109871.
- Kenmotsu H, Yamamoto N, Yamanaka T, Yoshiya K, Takahashi T, Ueno T, Goto K, Daga H, Ikeda N, Sugio K, et al. Randomized Phase III Study of Pemetrexed Plus Cisplatin Versus Vinorelbine Plus Cisplatin for completely resected stage II to IIIA Nonsquamous non-small-cell Lung Cancer. *J Clin Oncol.* 2020;38(19):2187–96.
- Shiraishi Y, Hakozaaki T, Nomura S, Kataoka T, Tanaka K, Miura S, Sekino Y, Ando M, Horinouchi H, Ohe Y, et al. A Multicenter, Randomized Phase III Study comparing platinum combination Chemotherapy Plus Pembrolizumab with Platinum Combination Chemotherapy Plus Nivolumab and Ipilimumab for Treatment-Naive Advanced non-small cell Lung Cancer without driver gene alterations: JCOG2007 (NIPPON Study). *Clin Lung Cancer.* 2022;23(4):e285–8.

11. Niho S, Kenmotsu H, Sekine I, Ishii G, Ishikawa Y, Noguchi M, Oshita F, Watanabe S, Nakajima R, Tada H, et al. Combination chemotherapy with irinotecan and cisplatin for large-cell neuroendocrine carcinoma of the lung: a multicenter phase II study. *J Thorac Oncol*. 2013;8(7):980–4.
12. Efferth T, Fu YJ, Zu YG, Schwarz G, Konkimalla VS, Wink M. Molecular target-guided tumor therapy with natural products derived from traditional Chinese medicine. *Curr Med Chem*. 2007;14(19):2024–32.
13. Yang XQ, Li CY, Xu MF, Zhao H, Wang D. Comparison of first-line chemotherapy based on irinotecan or other drugs to treat non-small cell lung cancer in stage IIIB/IV: a systematic review and meta-analysis. *BMC Cancer*. 2015;15:949.
14. Bai Y-P, Yang C-J, Deng N, Zhang M, Zhang Z-J, Li L, Zhou Y, Luo X-F, Xu C-R, Zhang B-Q, et al. Design and synthesis of novel 7-ethyl-10-fluoro-20-O-(cinnamic acid ester)-camptothecin derivatives as potential high selectivity and low toxicity topoisomerase I inhibitors for hepatocellular carcinoma. *Biochem Pharmacol*. 2022;200:115049.
15. Li M, Wang L, Wei Y, Wang W, Liu Z, Zuo A, Liu W, Tian J, Wang H. Anti-colorectal Cancer effects of a Novel Camptothecin Derivative PCC0208037 in Vitro and in vivo. *Pharmaceuticals*. 2023;16(1):53.
16. Du H, Huang Y, Hou X, Quan X, Jiang J, Wei X, Liu Y, Li H, Wang P, Zhan M, et al. Two novel camptothecin derivatives inhibit colorectal cancer proliferation via induction of cell cycle arrest and apoptosis in vitro and in vivo. *Eur J Pharm Sci*. 2018;123:546–59.
17. Zhou Y, Zhao H-Y, Jiang D, Wang L-Y, Xiang C, Wen S-P, Fan Z-C, Zhang Y-M, Guo N, Teng Y-O, et al. Low toxic and high soluble camptothecin derivative 2–47 effectively induces apoptosis of tumor cells in vitro. *Biochem Biophys Res Commun*. 2016;472(3):477–81.
18. Prasad Tharanga Jayasooriya RG, Dilshara MG, Neelaka Molagoda IM, Park C, Park SR, Lee S, Choi YH, Kim G-Y. Camptothecin induces G(2)/M phase arrest through the ATM-Chk2-Cdc25C axis as a result of autophagy-induced cytoprotection: implications of reactive oxygen species. *Oncotarget*. 2018;9(31):21744–57.
19. Chang A. Chemotherapy, chemoresistance and the changing treatment landscape for NSCLC. *Lung Cancer*. 2011;71(1):3–10.
20. Shahverdi M, Hajiasgharzadeh K, Sorkhabi AD, Jafarlou M, Shojaaee M, Tabrizi NJ, Alizadeh N, Santarpia M, Brunetti O, Safarpour H. The regulatory role of autophagy-related miRNAs in lung cancer drug resistance. *Biomed Pharmacother*. 2022;148:112735.
21. Zadeh FA, Raji A, Ali SA-J, Abdelbasset WK, Alekhina N, Iswanto AH, Terefe EM, Jalil AT. Autophagy-related chemoradiotherapy sensitivity in non-small cell lung cancer (NSCLC). *Pathology-Research Pract*. 2022;233:153823.
22. Zhang JW, Zhang SS, Song JR, Sun K, Zong C, Zhao QD, Liu WT, Li R, Wu MC, Wei LX. Autophagy inhibition switches low-dose camptothecin-induced premature senescence to apoptosis in human colorectal cancer cells. *Biochem Pharmacol*. 2014;90(3):265–75.
23. Chiu YH, Hsu SH, Hsu HW, Huang KC, Liu WT, Wu CY, Huang WP, Chen JYF, Chen BH, Chiu CC. Human non-small cell lung cancer cells can be sensitized to camptothecin by modulating autophagy. *Int J Oncol*. 2018;53(5):1967–79.
24. Saleh T, Cuttino L, Gewirtz DA. Autophagy is not uniformly cytoprotective: a personalized medicine approach for autophagy inhibition as a therapeutic strategy in non-small cell lung cancer. *Biochim Biophys Acta*. 2016;1860(10):2130–6.
25. Chou H-L, Lin Y-H, Liu W, Wu C-Y, Li R-N, Huang H-W, Chou C-H, Chiu S-J, Chiu C-C. Combination therapy of Chloroquine and C2-Ceramide enhances cytotoxicity in Lung Cancer H460 and H1299 cells. *Cancers (Basel)*. 2019;11(3):370.
26. Mizushima N. Autophagy: process and function. *Genes Dev*. 2007;21(22):2861–73.
27. Piekarski A, Khaldi S, Greene E, Lassiter K, Mason JG, Anthony N, Bottje W, Dridi S. Tissue distribution, gender- and genotype-dependent expression of autophagy-related genes in avian species. *PLoS ONE*. 2014;9(11):e112449.
28. Sui X, Chen R, Wang Z, Huang Z, Kong N, Zhang M, Han W, Lou F, Yang J, Zhang Q, et al. Autophagy and chemotherapy resistance: a promising therapeutic target for cancer treatment. *Cell Death Dis*. 2013;4:e838.
29. Li DD, Sun T, Wu XQ, Chen SP, Deng R, Jiang S, Feng GK, Pan JX, Zhang XS, Zeng YX, et al. The inhibition of autophagy sensitises colon cancer cells with wild-type p53 but not mutant p53 to topotecan treatment. *PLoS ONE*. 2012;7(9):e45058.
30. Liu F, Liu D, Yang Y, Zhao S. Effect of autophagy inhibition on chemotherapy-induced apoptosis in A549 lung cancer cells. *Oncol Lett*. 2013;5(4):1261–5.
31. Li JF, Huang RZ, Yao GY, Ye MY, Wang HS, Pan YM, Xiao JT. Synthesis and biological evaluation of novel aniline-derived asiatic acid derivatives as potential anticancer agents. *Eur J Med Chem*. 2014;86:175–88.
32. Zhang L, Li W, Xiao TF, Song ZH, Csuk R, Li SK. Design and Discovery of Novel Chiral Antifungal amides with 2-(2-Oxazolonyl)aniline as a Promising Pharmacophore. *J Agric Food Chem*. 2018;66(34):8957–65.
33. Almaawi A, Wang HT, Ciobanu O, Rowas SA, Rampersad S, Antoniou J, Mwale F. Effect of acetaminophen and nonsteroidal anti-inflammatory drugs on gene expression of mesenchymal stem cells. *Tissue Eng Part A*. 2013;19(7–8):1039–46.
34. Hillier SM, Marquis JC, Zayas B, Wishnok JS, Liberman RG, Skipper PL, Tannenbaum SR, Essigmann JM, Croy RG. DNA adducts formed by a novel antitumor agent 11 beta-dichloro in vitro and in vivo. *Mol Cancer Ther*. 2006;5(4):977–84.
35. Fedeles BI, Zhu AY, Young KS, Hillier SM, Proffitt KD, Essigmann JM, Croy RG. Chemical genetics analysis of an aniline mustard anticancer agent reveals complex I of the electron transport chain as a target. *J Biol Chem*. 2011;286(39):33910–20.
36. Behrends V, Giskeodegard GF, Bravo-Santano N, Letek M, Keun HC. Acetaminophen cytotoxicity in HepG2 cells is associated with a decoupling of glycolysis from the TCA cycle, loss of NADPH production, and suppression of anabolism. *Arch Toxicol*. 2019;93(2):341–53.
37. Lorincz T, Jemnitz K, Kardon T, Mandl J, Szarka A. Ferroptosis is involved in Acetaminophen Induced Cell Death. *Pathol Oncol Res*. 2015;21(4):1115–21.
38. Lee S, Lim MJ, Kim MH, Yu CH, Yun YS, Ahn J, Song JY. An effective strategy for increasing the radiosensitivity of human lung Cancer cells by blocking Nrf2-dependent antioxidant responses. *Free Radic Biol Med*. 2012;53(4):807–16.
39. Bonnet M, Flanagan JU, Chan DA, Lai EW, Nguyen P, Giaccia AJ, Hay MP. SAR studies of 4-pyridyl heterocyclic anilines that selectively induce autophagic cell death in Von Hippel-Lindau-deficient renal cell carcinoma cells. *Bioorg Med Chem*. 2011;19(11):3347–56.
40. Hundeshagen P, Hamacher-Brady A, Eils R, Brady NR. Concurrent detection of autolysosome formation and lysosomal degradation by flow cytometry in a high-content screen for inducers of autophagy. *BMC Biol*. 2011;9:38.
41. Wang Y, Peng RQ, Li DD, Ding Y, Wu XQ, Zeng YX, Zhu XF, Zhang XS. Chloroquine enhances the cytotoxicity of topotecan by inhibiting autophagy in lung cancer cells. *Chin J Cancer*. 2011;30(10):690–700.
42. Chen MC, Lee NH, Ho TJ, Hsu HH, Kuo CH, Kuo WW, Lin YM, Tsai FJ, Tsai CH, Huang CY. Resistance to irinotecan (CPT-11) activates epidermal growth factor receptor/nuclear factor kappa B and increases cellular metastasis and autophagy in LoVo colon cancer cells. *Cancer Lett*. 2014;349(1):51–60.
43. White E. The role for autophagy in cancer. *J Clin Invest*. 2015;125(1):42–6.
44. Chang WT, Bow YD, Chen YC, Li CY, Chen JY, Chu YC, Teng YN, Li RN, Chiu CC. The phenoxyphenol compound diTFPP mediates exogenous C2-Ceramide metabolism, inducing cell apoptosis accompanied by ROS formation and autophagy in Hepatocellular Carcinoma cells. *Antioxid (Basel)*. 2021;10(3):394.
45. Liu W, Wu CY, Lu MJ, Chuang YJ, Tsai EM, Leu S, Lin IL, Ko CJ, Chiu CC, Chang WT. The Phenoxyphenol Compound 4-HPPP Selectively Induces Antiproliferation Effects and Apoptosis in Human Lung Cancer Cells through Aneuployploidization and ATR DNA Repair Signaling. *Oxid Med Cell Longev*. 2020;2020:5167292.
46. Chang W-T, Liu W, Chiu Y-H, Chen B-H, Chuang S-C, Chen Y-C, Hsu Y-T, Lu M-J, Chiou S-J, Chou C-K, et al. A 4-Phenoxyphenol Derivative exerts Inhibitory effects on Human Hepatocellular Carcinoma Cells through regulating autophagy and apoptosis accompanied by downregulating  $\alpha$ -Tubulin expression. *Molecules*. 2017;22(5):854.
47. Chiu CC, Chou HL, Chen BH, Chang KF, Tseng CH, Fong Y, Fu TF, Chang HW, Wu CY, Tsai EM, et al. BPIQ, a novel synthetic quinoline derivative, inhibits growth and induces mitochondrial apoptosis of lung cancer cells in vitro and in zebrafish xenograft model. *BMC Cancer*. 2015;15:962.
48. Chiu C-C, Chen Y-C, Bow Y-D, Chen JY-F, Liu W, Huang J-L, Shu E-D, Teng Y-N, Wu C-Y, Chang W-T. diTFPP, a Phenoxyphenol, Sensitizes Hepatocellular Carcinoma Cells to C2-Ceramide-Induced autophagic stress by increasing oxidative stress and ER stress accompanied by LAMP2 hypoglycosylation. *Cancers (Basel)*. 2022;14(10):2528.
49. Paglin S, Hollister T, Delohery T, Hackett N, McMahlil M, Sphicas E, Domingo D, Yahlom J. A novel response of cancer cells to radiation involves autophagy and formation of acidic vesicles. *Cancer Res*. 2001;61(2):439–44.
50. Shubin AV, Demidyuk IV, Komissarov AA, Rafieva LM, Kostrov SV. Cytoplasmic vacuolization in cell death and survival. *Oncotarget*. 2016;7(34):55863–89.
51. Tanida I, Ueno T, Kominami E. LC3 and Autophagy. *Methods Mol Biol*. 2008;445:77–88.
52. Marínó G, Niso-Santano M, Baehrecke EH, Kroemer G. Self-consumption: the interplay of autophagy and apoptosis. *Nat Rev Mol Cell Biol*. 2014;15(2):81–94.

53. Zhang YB, Gong JL, Xing TY, Zheng SP, Ding W. Autophagy protein p62/SQSTM1 is involved in HAMLET-induced cell death by modulating apoptosis in U87MG cells. *Cell Death Dis.* 2013;4:e550.
54. Sevlever D, Jiang P, Yen SH. Cathepsin D is the main lysosomal enzyme involved in the degradation of alpha-synuclein and generation of its carboxy-terminally truncated species. *Biochemistry.* 2008;47(36):9678–87.
55. Hao W, Zhang X, Zhao W, Chen X. Psoralidin induces autophagy through ROS generation which inhibits the proliferation of human lung cancer A549 cells. *PeerJ.* 2014;2:e555.
56. Johnson-Cadwell LI, Jekabsons MB, Wang A, Polster BM, Nicholls DG. Mild uncoupling does not decrease mitochondrial superoxide levels in cultured cerebellar granule neurons but decreases spare respiratory capacity and increases toxicity to glutamate and oxidative stress. *J Neurochem.* 2007;101(6):1619–31.
57. Zhang F, Lau SS, Monks TJ. The cytoprotective effect of N-acetyl-L-cysteine against ROS-induced cytotoxicity is independent of its ability to enhance glutathione synthesis. *Toxicol Sci.* 2011;120(1):87–97.
58. Tat J, Liu M, Wen XY. Zebrafish cancer and metastasis models for in vivo drug discovery. *Drug Discov Today Technol.* 2013;10(1):e83–9.
59. Ali A, Goffin JR, Arnold A, Ellis PM. Survival of patients with non-small-cell lung cancer after a diagnosis of brain metastases. *Curr Oncol.* 2013;20(4):300–6.
60. Morth C, Valachis A. Single-agent versus combination chemotherapy as first-line treatment for patients with advanced non-small cell lung cancer and performance status 2: a literature-based meta-analysis of randomized studies. *Lung Cancer.* 2014;84(3):209–14.
61. Wu YJ, Neuwelt AJ, Muldoon LL, Neuwelt EA. Acetaminophen enhances cisplatin- and paclitaxel-mediated cytotoxicity to SKOV3 human ovarian carcinoma. *Anticancer Res.* 2013;33(6):2391–400.
62. Bondy SC. The Hormesis Concept: Strengths and Shortcomings. *Biomolecules.* 2023; 13(10).
63. Zielinski RR, Egl BJ, Chi KN. Targeting the apoptosis pathway in prostate cancer. *Cancer J.* 2013;19(1):79–89.
64. Chaabane W, User SD, El-Gazzah M, Jaksik R, Sajjadi E, Rzeszowska-Wolny J, Los MJ. Autophagy, apoptosis, mitoptosis and necrosis: interdependence between those pathways and effects on cancer. *Arch Immunol Ther Exp (Warsz).* 2013;61(1):43–58.
65. Broker LE, Krut FA, Giaccone G. Cell death independent of caspases: a review. *Clin Cancer Res.* 2005;11(9):3155–62.
66. Dalby KN, Tekedereli I, Lopez-Berestein G, Ozpolat B. Targeting the prodeath and prosurvival functions of autophagy as novel therapeutic strategies in cancer. *Autophagy.* 2010;6(3):322–9.
67. Kar R, Singha PK, Venkatachalam MA, Saikumar P. A novel role for MAP1 LC3 in nonautophagic cytoplasmic vacuolation death of cancer cells. *Oncogene.* 2009;28(28):2556–68.
68. Kroemer G, Levine B. Autophagic cell death: the story of a misnomer. *Nat Rev Mol Cell Biol.* 2008;9(12):1004–10.
69. Gewirtz DA. Autophagy, senescence and tumor dormancy in cancer therapy. *Autophagy.* 2009;5(8):1232–4.
70. Goehe RW, Di X, Sharma K, Bristol ML, Henderson SC, Valerie K, Rodier F, Davalos AR, Gewirtz DA. The autophagy-senescence connection in chemotherapy: must tumor cells (self) eat before they sleep? *J Pharmacol Exp Ther.* 2012;343(3):763–78.
71. Boya P. Lysosomal function and dysfunction: mechanism and disease. *Antioxid Redox Signal.* 2012;17(5):766–74.
72. Jung M, Lee J, Seo HY, Lim JS, Kim EK. Cathepsin inhibition-induced lysosomal dysfunction enhances pancreatic beta-cell apoptosis in high glucose. *PLoS ONE.* 2015;10(1):e0116972.
73. Xu CX, Zhao L, Yue P, Fang G, Tao H, Owonikoko TK, Ramalingam SS, Khuri FR, Sun SY. Augmentation of NVP-BE2253's anticancer activity against human lung cancer cells by blockage of autophagy. *Cancer Biol Ther.* 2011;12(6):549–55.
74. Trabbic CJ, Dietsch HM, Alexander EM, Nagy PI, Robinson MW, Overmeyer JH, Maltese WA, Erhardt PW. Differential induction of cytoplasmic vacuolization and methuosis by Novel 2-Indolyl-substituted pyridinylpropanones. *ACS Med Chem Lett.* 2014;5(1):73–7.
75. Hajiahmadi S, Lorzadeh S, Iranpour R, Karima S, Rajabibazi M, Shahsavari Z, Ghavami S. Temozolomide, Simvastatin and Acetylshikonin Combination induces mitochondrial-dependent apoptosis in GBM cells, which is regulated by Autophagy. *Biology (Basel).* 2023; 12(2).
76. McGlinchey RP, Lee JC. Cysteine cathepsins are essential in lysosomal degradation of alpha-synuclein. *Proc Natl Acad Sci U S A.* 2015;112(30):9322–7.
77. Seto S, Tsujimura K, Horii T, Koide Y. Autophagy adaptor protein p62/SQSTM1 and autophagy-related gene Atg5 mediate autophagosome formation in response to Mycobacterium tuberculosis infection in dendritic cells. *PLoS ONE.* 2013;8(12):e86017.
78. Tatti M, Motta M, Di Bartolomeo S, Scarpa S, Cianfanelli V, Cecconi F, Salvio R. Reduced cathepsins B and D cause impaired autophagic degradation that can be almost completely restored by overexpression of these two proteases in Sap C-deficient fibroblasts. *Hum Mol Genet.* 2012;21(23):5159–73.
79. Huang R, Liu W. Identifying an essential role of nuclear LC3 for autophagy. *Autophagy.* 2015;11(5):852–3.
80. Chen GY, Meng CL, Lin KC, Tuan HY, Yang HJ, Chen CL, Li KC, Chiang CS, Hu YC. Graphene oxide as a chemosensitizer: diverted autophagic flux, enhanced nuclear import, elevated necrosis and improved antitumor effects. *Biomaterials.* 2015;40:12–22.
81. Kaur J, Debnath J. Autophagy at the crossroads of catabolism and anabolism. *Nat Rev Mol Cell Biol.* 2015;16(8):461–72.
82. Hah YS, Noh HS, Ha JH, Ahn JS, Hahm JR, Cho HY, Kim DR. Cathepsin D inhibits oxidative stress-induced cell death via activation of autophagy in cancer cells. *Cancer Lett.* 2012;323(2):208–14.
83. Gibson SB. Investigating the role of reactive oxygen species in regulating autophagy. *Methods Enzymol.* 2013;528:217–35.
84. Filomeni G, De Zio D, Cecconi F. Oxidative stress and autophagy: the clash between damage and metabolic needs. *Cell Death Differ.* 2015;22(3):377–88.
85. Chen Y, Azad MB, Gibson SB. Superoxide is the major reactive oxygen species regulating autophagy. *Cell Death Differ.* 2009;16(7):1040–52.
86. Liu Y, Levine B. Autosis and autophagic cell death: the dark side of autophagy. *Cell Death Differ.* 2015;22(3):367–76.
87. Ma K, Zhang C, Huang MY, Li WY, Hu GQ. Cinobufagin induces autophagy-mediated cell death in human osteosarcoma U2OS cells through the ROS/JNK/p38 signaling pathway. *Oncol Rep.* 2016;36(1):90–8.
88. MacRae CA, Peterson RT. Zebrafish as tools for drug discovery. *Nat Rev Drug Discov.* 2015;14(10):721–31.
89. Nakamura S, Yoshimori T. New insights into autophagosome-lysosome fusion. *J Cell Sci.* 2017;130(7):1209–16.
90. Chiu CC, Chen YC, Bow YD, Chen JY, Liu W, Huang JL, Shu ED, Teng YN, Wu CY, Chang WT. diTFPP, a Phenoxyphenol, Sensitizes Hepatocellular Carcinoma Cells to C(2)-Ceramide-Induced autophagic stress by increasing oxidative stress and ER stress accompanied by LAMP2 hypoglycosylation. *Cancers (Basel).* 2022; 14(10).
91. Kaizuka T, Morishita H, Hama Y, Tsukamoto S, Matsui T, Toyota Y, Kodama A, Ishihara T, Mizushima T, Mizushima N. An autophagic Flux probe that releases an Internal Control. *Mol Cell.* 2016;64(4):835–49.
92. Tanaka H, Hino H, Moriya S, Kazama H, Miyazaki M, Takano N, Hiramoto M, Tsukahara K, Miyazawa K. Comparison of autophagy inducibility in various tyrosine kinase inhibitors and their enhanced cytotoxicity via inhibition of autophagy in cancer cells in combined treatment with azithromycin. *Biochem Biophys Rep.* 2020;22:100750.

## Publisher's note

Springer Nature remains neutral with regard to jurisdictional claims in published maps and institutional affiliations.